Journal of Solid Mechanics **1** (2009) 45-57

Mechanical Behavior of an Electrostatically-Actuated Microbeam under Mechanical Shock

M. Fathalilou[1], A. Motallebi[2], H. Yagubizade[3], Gh. Rezazadeh[3,*], K. Shirazi[1], Y. Alizadeh[1]

[1]*Sama Organization (Affiliated with Islamic Azad University), Khoy Branch, Iran*
[2]*Department of Mechanical Engineering, Islamic Azad University, Khoy Branch, Khoy, Iran*
[3]*Department of Mechanical Engineering, Urmia University, Urmia, Iran*

Received 19 February 2009; accepted 25 April 2009

ABSTRACT
In this paper static and dynamic responses of a fixed-fixed microbeam to electrostatic force and mechanical shock for different cases have been studied. The governing equations whose solution holds the answer to all our questions about the mechanical behavior is the nonlinear elasto-electrostatic equations. Due to the nonlinearity and complexity of the derived equations analytical solution are not generally available; therefore, the obtained differential equations have been solved by using of a step by step linearization method (SSLM) and a Galerkin based reduced order model. The pull-in voltage of the structure and the effect of shock forces on the mechanical behavior of undeflected and electrostatically deflected microbeam have been investigated. The proposed models capture the other design parameters such as intrinsic residual stress from fabrication processes and the nonlinear stiffening or stretching stress due to beam deflection.

Keywords: MEMS; Microbeam; Electrostatic actuation; Pull-in voltage; Mechanical shock

1 INTRODUCTION

MICROELECTROMECHANICAL systems (MEMS) are increasingly gaining popularity in modern technologies, such as atomic force microscope (AFM), sensing sequence-specific DNA, and detection of single electron spin, mass sensors, chemical sensors, and pressure sensors [1–4]. MEMS devices are generally classified according to their actuation mechanisms. Actuation mechanisms for MEMS vary depending on the suitability to the application at hand. The most common actuation mechanisms are electrostatic, pneumatic, thermal, and piezoelectric [5]. Electrostatically actuated devices form a broad class of MEMS devices due to their simplicity, as they require few mechanical components and small voltage levels for actuation [5], which the electrostatic actuation is inherently non-linear. Microbeams (e.g., fixed-fixed and cantilever microbeams) under voltage driving are widely used in many MEMS devices such as capacitive micro-switches and resonant micro-sensors. These devices are fabricated, to some extent, in a more mature stage than some other MEMS devices. Fixed-fixed microbeams due to their high natural frequencies are widely used in resonant sensors and actuators. One of the most important issues in the electrostatically-actuated micro-devices is the pull-in instability. The pull-in instability is a discontinuity related to the interplay of the elastic and electrostatic forces. When a potential difference is applied between a conducting structure and a ground level, the structure deforms due to electrostatic forces. The elastic forces grow about linearly with displacement whereas the electrostatic forces grow inversely proportional to the square of the distance. When the voltage is increased the displacement grows until at one point the growth rate of the electrostatic force exceeds than the elastic force and the system cannot reach a force balance without a physical contact, thus pull-in instability occurs. The critical voltage is known as "pull-in voltage". Some previous studies predicted pull-in phenomena based on static analysis by considering static application of a DC voltage [6-9].

* Corresponding author.
E-mail address: g.rezazadeh@urmia.ac.ir (Gh. Rezazadeh).

Mechanical shock is one of the most critical parameters which is directly related to MEMS reliability, so it must be studied sufficeintly. MEMS devices can be exposed to shock during fabrication, deployment and operation. Some problems such as cracking, chipping and fracture due to mechanical shock which have dramatic influence on reliability and so long term stability of these kind of devices and it can also cause damage due to severe motion of portions of the device, which may lead to mechanical and/or electrical failure [10]. Mechanical shock loads can cause microstructures such as microbeams, to hit the stationary electrodes underneath them, causing stiction [11] and short circuit problems [12] and hence failure it. Failure in MEMS devices can occur through stiction and electric short circuits due to contacts between movable and stationary electrodes. The most cases of MEMS devices are fabricated of silicon or polysilicon, so, they have high toughness against stretching stresses due to shock loads. But when they hit substrate, they can be broken due to the contact stresses. A shock can be defined as a force applied suddenly and over a short period of time relative to the natural period of the structure [13] and a shock load pulse can be characterized by maximum value, duration and shape. MEMS devices response to mechanical shock has been studied by several researches. The response of commercial accelerometers to shock loads has experimentally been studied by Beliveau et al. [14] and reported some unexpected results. Brown et al. [15] subjected commercial accelerometers and a pressure sensor to high-tests. They could not receive suitable results and suggested that an improved dynamic model of MEMS devices under shock load is needed. Lim et al. [16] studied the effects of shock on a MEMS actuator using the FE software ANSYS. Wagner et al. [17] studied the response of a MEMS accelerometer to a shock load induced by a drop test. They used the linear beam theory, for rough estimations and FE analysis to calculate the stress history of the device during impact. Fan and Shaw [18] simulated the response of a comb-drive accelerometer subjected to severe dynamic shock loads in all directions using an FE model in software ABAQUS. They remarked that this problem requires a highly non-linear transient dynamic analysis, which is computationally very expensive. Li and Shemansky [19] studied the motion of MEMS accelerometers during drop tests. They used a single-degree-of-freedom (SDOF) model and a continuous system beam model to account for the flexibility of the structures and calculated their maximum deflection. Srikar and Senturia [20] modeled microstructures using an undamped SDOF model attached to an accelerating base. Yee et al. [21] and Millet et al. [22] analyzed the behavior of fixed-fixed microbeams under shock loads. They used a linear beam model for small-deflection cases and Raleigh-Ritz technique for large-deflection cases and indicated that their solution is not numerically accurate even for small deflections. Tas et al. [11] identified electrostatic and acceleration forces during shock as two possible causes of the contact of the microstructures during the operation of the MEMS devices, but they did not study the simultaneous effect of electrostatic forces and mechanical shock loadings. Coster et al. [23] modeled the behavior of the RF MEMS switch actuated by an electrostatic force subjected to shock using a SDOF model. From the aforesaid background, it is understood that there is an insufficiency in the study of MEMS devices response under simultaneous effects of the electrostatic forces with mechanical shock loading.

In this paper Galerkin based step by step linearization method (SSLM) and reduced order model, have been used based on a continuous beam model to investigate the static and dynamic response of MEMS devices employing fixed-fixed beams. Initially, it is focused on the static electrostatic loading considering the effects of stretching and residual stresses and investigating the static pull-in of the structure. Next, the dynamic response of an electrostatically deflected microbeam under different shock types with different shock durations and amplitudes is studied. It is presented as a complete solution for the shock problem of a fixed-fixed microbeam for the cases of half-sine shock pulse, saw-tooth shock pulse and rectangular shock pulse. Also combination of electrostatic force and half-sine shock pulse on the shifting of the pull-in voltage has been studied.

2 NONLINEAR DISTRIBUTED ELECTROMECHANICAL COUPLED MODEL

Fixed-fixed microbeams are of primary interest here (see Fig. 1) that the work is easily extendable to cantilevered beams. Capacitively-actuated microbeam is a suspended elastic beam with an applied electrostatic force. The device consists of a plate, called the ‘‘beam’’, suspended over a dielectric film deposited on top of the center conductor and fixed at both ends to the ground conductor. When a voltage is applied between the beam and substrate, the attractive electrostatic pressure pulls the beam down towards the dielectric film. The dielectric film serves to prevent stiction between the beam and substrate, and yet provides a low impedance path between the two contacts.

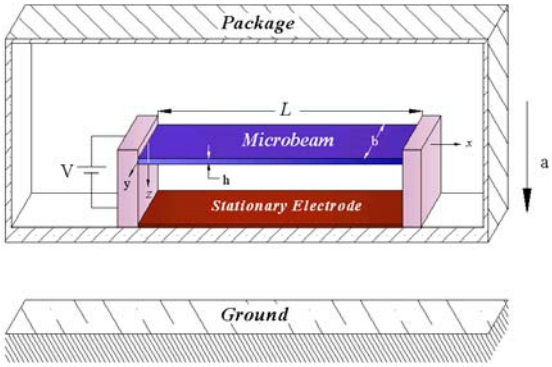

Fig. 1
Schematic view of an electrostatically actuated fixed-fixed microbeam.

The governing equation of motion for the transverse displacement of the beam $w(x,t)$ actuated by a mechanical shock and an electrostatic load of voltage V is written as:

$$\widetilde{E}I\frac{\partial^4 w}{\partial x^4}+\rho bh\left(\frac{\partial^2 w}{\partial t^2}-a\right)+c\frac{\partial w}{\partial t}=\frac{\varepsilon b}{2}\left(\frac{V}{d-w(x,t)}\right)^2 \tag{1}$$

where $\widetilde{E}$ is dependent on the beam width b and film thickness h. A beam is considered wide when $b\geq 5h$. Wide beams exhibit plane-strain conditions, and therefore, $\widetilde{E}$ becomes the plate modulus $E/(1-\upsilon^2)$, where E and υ are the Young's modulus and Poisson's ratio, respectively. A beam is considered narrow when $b<5h$. In this case, $\widetilde{E}$ simply becomes the Young's modulus, E. $I=(bh^3/12)$ is the effective moment of inertia of the cross-section which is wide relative to thickness and width, ρ is density, ε and d are the dielectric constant of the gap medium and initial gap, respectively. The microbeam is subject to a viscous damping, which can be due to squeeze-film damping. This effect is approximated by an equivalent damping coefficient c per unit length [9], a is the package acceleration created by a mechanical shock force due to dropping of the package ($a=a_0 g(t)$) where a_0 is the amplitude of the shock pulse and $g(t)$ is the shape of it. The fixed-fixed beam's boundary conditions are given by:

$$w(0,t)=w(L,t)=0,\quad \frac{\partial w}{\partial x}(0,t)=\frac{\partial w}{\partial x}(L,t)=0 \tag{2}$$

2.1. Stretching Stress Effect

Fixed-fixed microbeams represent an example of microstructure suffering from the geometric nonlinearity mid-plane stretching. When a beam is in bending, the actual beam length L' is longer than the original length L, although there is no displacement in the x direction at the beam ends. The actual length along the center line of the beam is calculated by integrating the arc length $\mathrm{d}s$ along the curved beam based on the cubic shape functions for small deflection of beam, $w(x)$:

$$L'=\int_0^L \mathrm{d}s\approx\int_0^L\sqrt{1+\left(\frac{\mathrm{d}w}{\mathrm{d}x}\right)^2}\,\mathrm{d}x \tag{3}$$

Considering $L>>w$, hence $(\mathrm{d}w/\mathrm{d}x)^2<<1$, as a result, the elongation is approximately given by:

$$\Delta L \approx \frac{1}{2}\int_0^L \left(\frac{\mathrm{d}w}{\mathrm{d}x}\right)^2 \mathrm{d}x \tag{4}$$

Therefore the stretching stress and force is given by:

$$\sigma_a = \frac{\widetilde{E}}{2L}\int_0^L \left(\frac{\mathrm{d}w}{\mathrm{d}x}\right)^2 \mathrm{d}x, \quad \text{and} \quad N_a = bh\sigma_a \tag{5}$$

2.2. Residual Stress Effect

Residual stress, due to the inconsistency of both the thermal expansion coefficient and the crystal lattice period between the substrate and thin film, is unavoidable in surface micromachining techniques. Accurate and reliable data for residual stress are crucial to the proper design of MEMS devices that are related to these techniques [24, 25]. Considering the fabrication sequence of MEMS devices, residual force can be expressed as:

$$N_r = \sigma_r(1-\upsilon)bh \tag{6}$$

where σ_r is the biaxial residual stress [26], and υ is the Poisson's ratio. Assuming the stretching and residual stresses effects, the governing differential equation takes the following form:

$$\widetilde{E}I\frac{\partial^4 w}{\partial x^4} + \rho bh\left(\frac{\partial^2 w}{\partial t^2} - a\right) + c\frac{\partial w}{\partial t} - \left[N_a + N_r\right]\frac{\partial^2 w}{\partial x^2} = \frac{\varepsilon b}{2}\left(\frac{V}{d - w(x,t)}\right)^2 \tag{7}$$

For convenience in analysis, this equation must be non-dimensionalized. In particular, both the transverse displacement, w, and the spatial coordinate, x, are normalized by characteristic lengths of the system and the gap size and beam length, respectively, according to: $\hat{w} = w/d$ and $\hat{x} = x/L$. Time is non-dimensionalized by a characteristic period of the system according to: $\hat{t} = t/t^*$ with $t^* = (\rho bhL^4/\widetilde{E}I)^{1/2}$.

Substituting these parameters into Eq. (7), the following nondimensional equation is obtained:

$$\frac{\partial^4 \hat{w}}{\partial \hat{x}^4} + \frac{\partial^2 \hat{w}}{\partial \hat{t}^2} + \hat{c}\frac{\partial \hat{w}}{\partial \hat{t}} - \left[\hat{N}_a + \hat{N}_r\right]\frac{\partial^2 \hat{w}}{\partial \hat{x}^2} = \alpha_1\left(\frac{V}{1-\hat{w}(\hat{x},\hat{t})}\right)^2 + \alpha_2 g(\hat{t}) \tag{8}$$

The non-dimensional parameters appeared in Eq. (8) are:

$$\alpha_1 = \frac{6\varepsilon L^4}{\widetilde{E}h^3 d^3}, \quad \alpha_2 = \frac{12\rho a_0 L^4}{\widetilde{E}dh^2}, \quad \hat{c} = \frac{12cL^4}{\widetilde{E}bh^3 t^*}, \quad \hat{N}_a = \frac{12N_a L^2}{\widetilde{E}bh^3}, \quad \hat{N}_r = \frac{12N_r L^2}{\widetilde{E}bh^3} \tag{9}$$

3 NUMERICAL SOLUTIONS

3.1. Static Analysis

In the static analysis there is no exist time derivatives and the shock forcing term, so using Eq. (8) the governed equation describing the static deflection of the microbeam can be obtained as follow:

$$L(\hat{w}_s, V) = \frac{\mathrm{d}^4 \hat{w}_s}{\mathrm{d}\hat{x}^4} - \left[\hat{N}_a + \hat{N}_r\right]\frac{\mathrm{d}^2 \hat{w}_s}{\mathrm{d}\hat{x}^2} - \alpha_1\left(\frac{V}{1-\hat{w}_s(\hat{x})}\right)^2 = 0 \tag{10}$$

where the $\hat{w}_s(\hat{x})$ for fixed-fixed end microbeam must be satisfied same boundary condition as mentioned in Eq. (2). Due to the nonlinearity of derived equation, the solution is complicated and time consuming. Direct applying Galerkin based reduced order model create a set of nonlinear algebraic equation. In this paper we use a method to solve it which consists of two steps. In first step, we use step by step linearization method (SSLM), and in second, Galerkin method for solving the linear obtained equation is used. Because of considerable value of $\hat{w}$ respect to initial gap especially when the applied voltage increases, the linearizing respect to $\hat{w}$, may causes some considerable errors, therefore, to minimize the value of errors, the method of step-by-step applied voltage increasing is proposed and the governing equation is linearized at each step [27].

To use SSLM, it is supposed that the $\hat{w}_s^k$, is the displacement of beam due to the applied voltage V^k. Therefore, by increasing the applied voltage to a new value, the displacement can be written as:

$$\hat{w}_s^{k+1} = \hat{w}_s^k + \delta\hat{w} = \hat{w}_s^k + \psi(\hat{x}) \tag{11}$$

when

$$V^{k+1} = V^k + \delta V \tag{12}$$

Therefore, Eq. (10) can be rewritten as follow:

$$\frac{\mathrm{d}^4 \hat{w}_s^{k+1}}{\mathrm{d}\hat{x}^4} - \left[\hat{N}_a^{k+1} + \hat{N}_r\right]\frac{\mathrm{d}^2 \hat{w}_s^{k+1}}{\mathrm{d}\hat{x}^2} = \alpha_1\left(\frac{V^{k+1}}{1-\hat{w}_s^{k+1}}\right)^2 \tag{13}$$

By considering small value of δV, it is expected that ψ would be small enough, hence using of Calculus of Variation Theory and Taylor's series expansion about $\hat{w}^k$, and applying the truncation to first order of it for suitable value of δV, it is possible to obtain desired accuracy. The linearized equation to calculate ψ can be expressed as:

$$L(\psi) = \frac{\mathrm{d}^4 \psi}{\mathrm{d}\hat{x}^4} - \left[\hat{N}_a^k + \delta\hat{N}_a + \hat{N}_r\right]\frac{\mathrm{d}^2 \psi}{\mathrm{d}\hat{x}^2} - \delta\hat{N}_a \left.\frac{\mathrm{d}^2 \hat{w}}{\mathrm{d}\hat{x}^2}\right|_{(\hat{w}^k, V^k)} - 2\alpha_1 \frac{(V^k)^2}{(1-\hat{w}_s^k)^3}\psi - 2\alpha_1 \frac{V^k \delta V}{(1-\hat{w}_s^k)^2} = 0 \tag{14}$$

where variation of the hardening term based on Calculus Variation Theory can be expressed as:

$$\delta\hat{N}_a = \int_0^1 \left(\left.\frac{\mathrm{d}^2 \hat{w}}{\mathrm{d}\hat{x}^2}\right|_{(\hat{w}^k, V^k)}\right)\psi(\hat{x})\,\mathrm{d}\hat{x} \tag{15}$$

By considering small value of $\delta\hat{V}$ and as a result $\psi(\hat{x})$, multiplying $\delta\hat{N}_a$ to $\mathrm{d}^2\psi/\mathrm{d}\hat{x}^2$ would be small enough that can be neglected. The obtained linear differential equation is solved by Galerkin based reduced order model. $\psi(\hat{x})$ based on function spaces can be expressed as:

$$\psi(\hat{x}) = \sum_{j=1}^{\infty} a_j\, \phi_j(\hat{x}) \tag{16}$$

where $\phi_i(\hat{x})$ is the *i*th shape function that satisfies the boundary conditions. The unknown $\psi(\hat{x})$, is approximated by truncating the summation series to a finite number, *n*:

$$\psi_n(\hat{x}) = \sum_{j=1}^{n} a_j \, \phi_j(\hat{x}) \tag{17}$$

By substituting the Eq. (17) into Eq. (14), and multiplying by $\phi_i(\hat{x})$ as a weight function in Galerkin method and then integrating the outcome from $\hat{x} = 0$ to 1, the Galerkin based reduced-order model is generated.

3.2. Dynamic Analysis

To study the fixed-fixed microbeam response to dynamic loading a Galerkin-based reduced order model can be used [28]. Because of the non-linearity of the stretching and electrostatic force terms, direct applying of reduced order model to dynamic equation (Eq. (8)) leads to generation of *n* nonlinear coupled ordinary differential equation and consequently the solution is more complicated. To solve this difficulty, the hardening $(\hat{N}_a)$ and forcing terms in Eq. (8) are considered a constant term in each time step of integration and takes the value of previous step. By selecting small enough time steps this assumption leads to accurate enough results. Now Eq. (8) can be rewritten as following:

$$\frac{\partial^4 \hat{w}}{\partial \hat{x}^4} + \frac{\partial^2 \hat{w}}{\partial \hat{t}^2} + \hat{c}\frac{\partial \hat{w}}{\partial \hat{t}} - \left[\ddot{\hat{N}}_a + \hat{N}_r\right]\frac{\partial^2 \hat{w}}{\partial \hat{x}^2} = F(\hat{V}, \ddot{\hat{w}}, g) \tag{18}$$

To achieve a reduced order model, $\hat{w}(\hat{x},\hat{t})$ can be approximated as:

$$\hat{w}(\hat{x},\hat{t}) = \sum_{j=1}^{n} T_j(\hat{t}) \, \phi_j(\hat{x}) \tag{19}$$

By substituting the Eq. (19) into Eq. (18) and multiplying by $\phi_i(\hat{x})$ as a weight function in Galerkin method and then integrating the outcome from $\hat{x} = 0$ to 1, the Galerkin based reduced order model is generated as:

$$\sum_{j=1}^{n} M_{ij}\ddot{T}_j(\hat{t}) + \sum_{j=1}^{n} C_{ij}\dot{T}_j(\hat{t}) + \sum_{j=1}^{n} (K_{ij}^m + K_{ij}^a)T_j(\hat{t}) = F_i \tag{20}$$

where M, C, K^m and K^a are mass, damping, mechanical and axial stiffness matrices, respectively. Also F introduces the forcing vector. The mentioned matrices and vector are given by:

$$M_{ij} = \int_0^1 \phi_i \phi_j \, \mathrm{d}\hat{x} \qquad C_{ij} = \hat{c}\int_0^1 \phi_i \phi_j \, \mathrm{d}\hat{x} \qquad i,j=1,\ldots,n$$

$$K_{ij}^m = \int_0^1 \phi_i \phi_j{}^{iv} \, \mathrm{d}\hat{x} \qquad K_{ij}^a = -(\ddot{\hat{N}}_a + \hat{N}_r)\int_0^1 \phi_i \phi_j'' \, \mathrm{d}\hat{x} \qquad F_i = \int_0^1 \phi_i F(\hat{V}, \ddot{\hat{w}}, g) \, \mathrm{d}\hat{x} \tag{21}$$

Now, Eq. (20) can be integrated over time by various numerical integration methods where $\ddot{\hat{N}}_a$ and $\ddot{\hat{w}}(\hat{x},\hat{t})$ in each time step of integration take the value of previous step.

4 NUMERICAL RESULTS AND DISCUSSION

4.1. Microbeam behavior under static electrostatic load

The pull-in results for a fixed-fixed microbeam obtained from our proposed method are compared with the results predicted in [7] and [8]. The fixed-fixed microbeam's geometric and material properties are given as follows [8]: Young's modulus E is 169 GPa, Poisson's ratio is 0.06, width of the beam b is $50\,\mu m$ for the simple beam, beam thickness h is $3\,\mu m$, initial gap d is $1\,\mu m$, and the permittivity of air is 8.85 pF/m. The results of Tables 1 and 2 indicate that pull-in voltages calculated from the proposed method agree well with the results calculated from the predicted results by GDQM algorithm [7] and the 2-D distributed model and the 3-D MEMCAD model [8].

4.2. Microbeam behavior under dynamic loadings

As a case study, the geometric and material properties of the fixed-fixed microbeam in all following sections are: the length of the beam L is $900\,\mu m$, the width of the beam b is $100\,\mu m$, Young's modulus $\widetilde{E}$ is $169\,Gpa$, the thickness h is $1.5\,\mu m$, the initial gap d is $2\,\mu m$ and the permittivity of air ε is 8.85 pF/m. The pull-in voltage of this structure based on SSLM static analysis is 3.45 V that in the following sections, the pull-in instability based on some other conditions has been studied.

4.2.1. Mechanical shock loading on the undeflected microbeam

In this section, the dynamic behavior of the microbeam under a shock load is studied. The shock profile $g(t)$ can be approximated as a half-sine, a saw-tooth, or a rectangular pulse [29]. These pulses are expressed mathematically as:

For half-sine pulse: $g(t) = \sin\left(\frac{\pi}{T}t\right)\{H(t) - H(t-T)\}$

For saw-tooth pulse: $g(t) = 2\{r(t) - 2r(t-T/2) + r(t-T)\}/T$

For rectangular pulse: $g(t) = H(t) - H(t-T)$

where T is the shock duration and $H(t)$ is the unit step function, and $r(t)$ is the unit ramp function. The duration of this pulse can vary from 0.1 to 1.0 ms, which spans all the possible durations of the shock pulse in the case of a hard-floor drop test [29].

Table 1
Comparison of calculated pull-in voltages for fixed-fixed beams with $L = 250\,\mu m$

Residual Stress (MPa)	0	100	-25
V proposed model (SSLM)	39.42	57.65	33.49
V (GDQM) [7]	39.13	57.62	33.63
V (2D) [8]	39.50	56.90	33.70
V (MEMCAD) [8]	40.10	57.60	33.60

Table 2
Comparison of calculated pull-in voltages for fixed-fixed beams with $L = 350\,\mu m$

Residual Stress (MPa)	0	100	-25
V proposed model (SSLM)	20.12	36.02	13.53
V (GDQM) [7]	20.36	35.99	13.60
V (2D) [8]	20.20	35.40	13.80
V (MEMCAD) [8]	20.30	35.80	13.70

Figs. 2a and 2b depict the time response of the microbeam under a 1000g half-sine shock pulse for the cases of $T=1.0$ and $T=0.1\,\text{ms}$, respectively. In Figs. 2c and 2d, the micro beam is subjected to a 500g half-sine shock pulse in $T=1.0$ and $T=0.1\,\text{ms}$ and in Figs. 3a and 3b a 1000g saw-tooth shock pulse is applied to the microbeam. It should be pointed out that all above cases are in no damping case. Figs. 3c and 3d show the dynamic behavior of the microbeam subjected to rectangular shock pulse in $T=1.0$ and $T=0.1\,\text{ms}$. With attention to the response of the microbeam to shock load in 0.1 ms duration, which is close to the natural period of the microbeam, it can be seen that the maximum amplitude of the microbeam is larger than that subjected to shock pulse in 1 ms duration. It is noted that the maximum amplitude of the microbeam in rectangular shock pulse is larger than the cases of saw-tooth and half-sine shock pulses but saw-tooth and half-sine cases are in the same range.

As mentioned in previous works [16, 29], the half-sine shape is a good representation for the shape of the actual shock pulse. So, is assumed the shock profile to be a half-sine in the next sections. Figs. 4a and 4b depict the effect of stretching stresses in the response of the microbeam versus shock amplitude in no damping case in two different shock durations. It is noted that by considering stretching stress effect in the governed equation, the microbeam deflection changes non-linearly with the shock amplitude and without this effect, it changes linearly. As shown, in small shock amplitudes, the effect of stretching is negligible but in higher shocks this effect is considerable. In Fig. 5, the effect of residual stresses on the microbeam response to shock pulse is investigated. As seen, when the residual stress increases, the microbeam becomes more resistant to shock because it gets stiffer. Figs. 6a and 6b compare the response of the microbeam for different damping ratios in the case of $T=1.0\,\text{ms}$ and $T=0.1\,\text{ms}$, respectively.

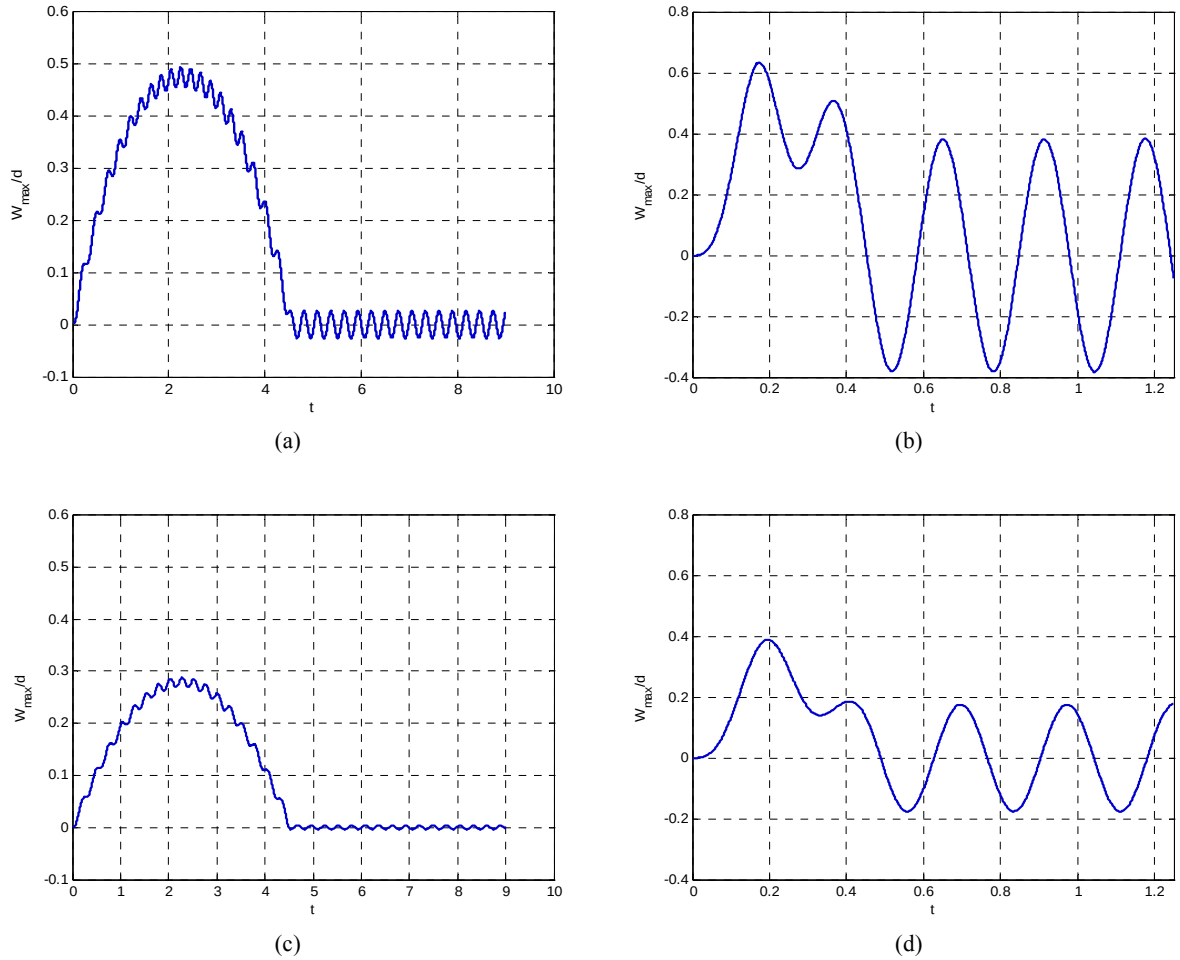

Fig. 2
Time history of undamped response of the microbeam subjected to half-sine shock pulse; (a): 1000g shock amplitude, *T*=1 ms; (b): 1000g shock amplitude, *T*=0.1 ms; (c): 500g shock amplitude, *T*=1 ms; (d): 500g shock amplitude, *T*=0.1 ms.

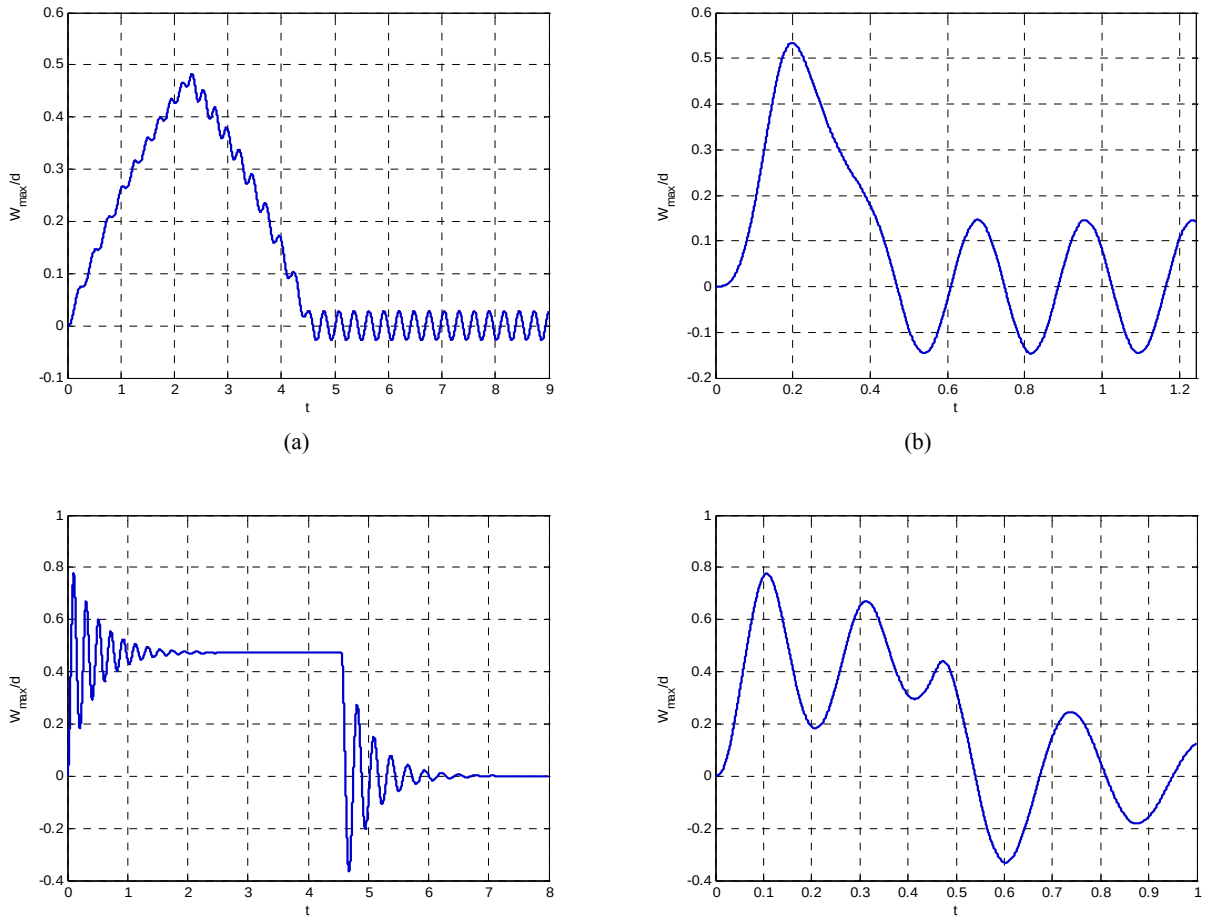

Fig. 3
Time history of the undamped response of the microbeam subjected to saw-tooth shock pulse; (a): T=1 ms; (b): T=0.1 ms and rectangular pulse; (c): T=1 ms; (d): T=0.1 ms with 1000g shock amplitude.

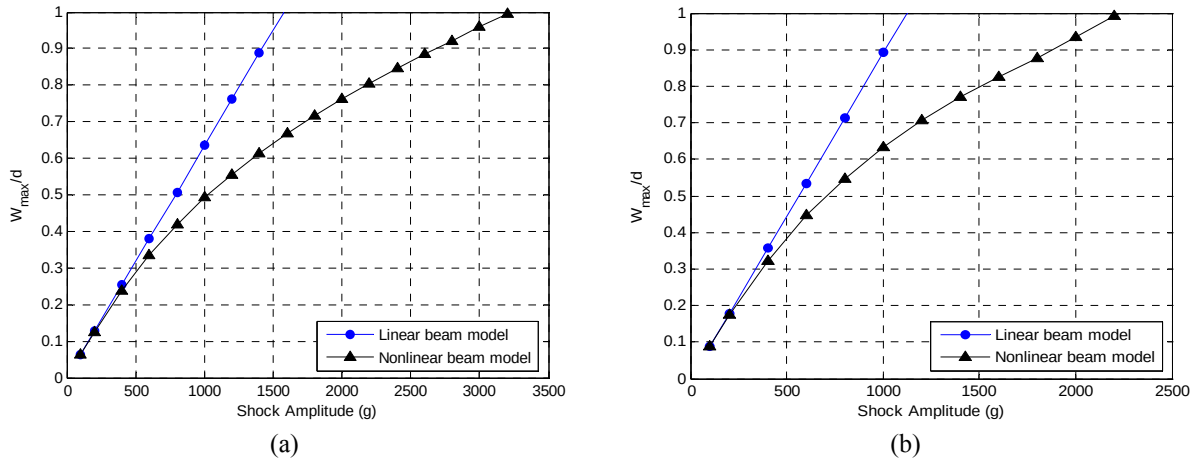

Fig. 4
The difference between the linear and nonlinear model of the microbeam in $\zeta = 0$; (a) T=1 ms; (b): T=0.1 ms.

In the case of $T=1.0$ ms, the response for no damping and damping ratio of 0.1 are compared and as seen, when the shock amplitude increases, damping parameter becomes considerable. In the case of $T=0.1$ ms, because of the $\zeta=0.1$ cannot enough damp small oscillations of the microbeam in shock durations; the effect of damping is considerable up to higher damping ratios.

4.2.2. Mechanical shock loading on electrostatically deflected microbeam

When the shock load is applied to the electrostatically deflected microbeam, the governed equation can be written as:

$$\frac{\partial^4 \hat{w}}{\partial \hat{x}^4}+\frac{\partial^2 \hat{w}}{\partial \hat{t}^2}+\hat{c}\frac{\partial \hat{w}}{\partial \hat{t}}-\left[\hat{N}_a+\hat{N}_r\right]\frac{\partial^2 \hat{w}}{\partial \hat{x}^2}=\alpha_1\left(\frac{V}{1-\hat{w}(\hat{x},\hat{t})}\right)^2+\alpha_2 g(\hat{t}) \tag{22}$$

The initial condition of the electrostatically deflected microbeam is: $\hat{w}(\hat{x},0)=\hat{w}_s(\hat{x})$. By comparing Figs. 7a and 7b, it is clear that 2.10 V is the pull-in voltage in this type of actuation and with attention to Figs. 8a and 8b, it can be gained that 1.75 V is the pull-in voltage in 0.1 ms shock duration case.

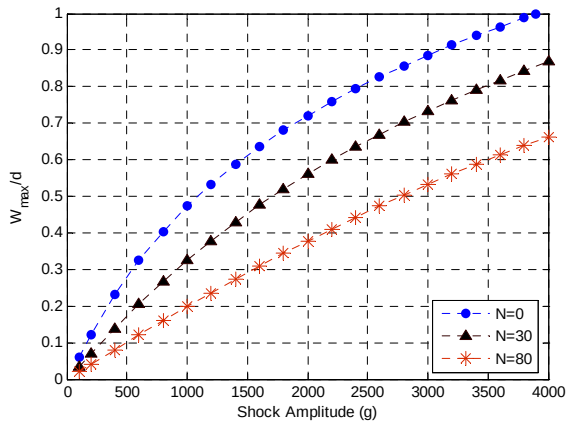

Fig. 5
Response of the microbeam subjected to half-sine shock pulse for different residual stresses in $\zeta=0$.

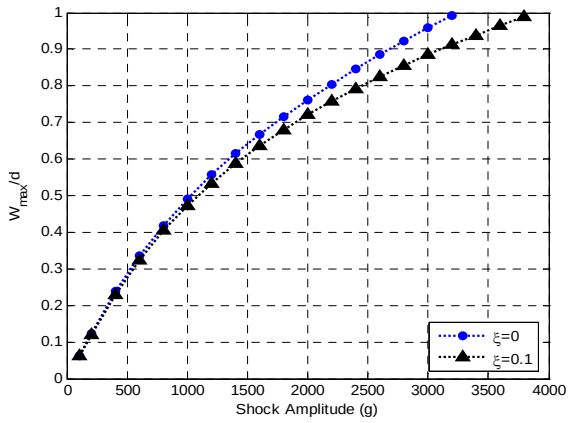

(a)

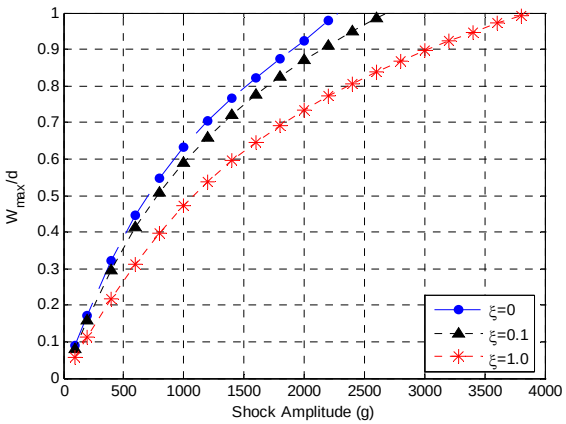

(b)

Fig. 6
Maximum deflection of the microbeam subjected to half-sine shock for various damping ratios; (a): *T*=1 ms; (b): *T*=0.1 ms.

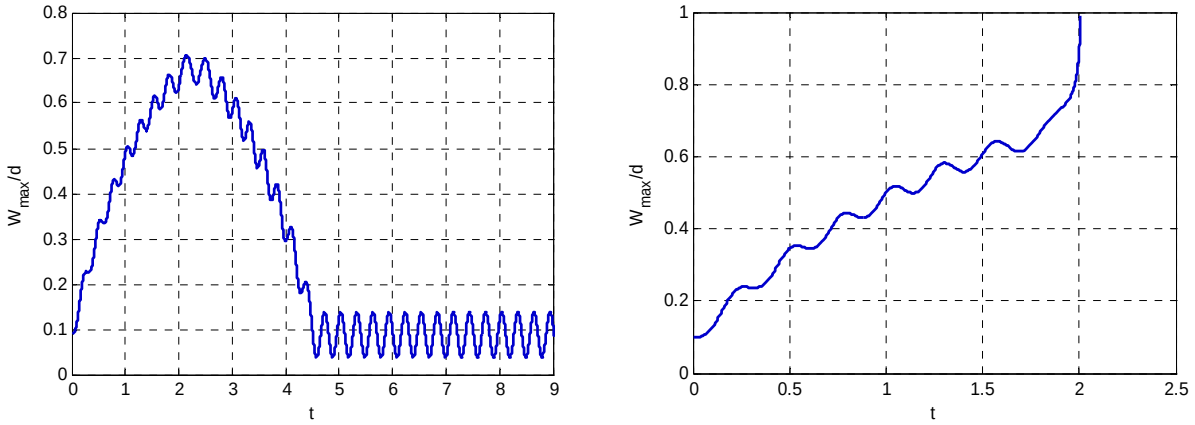

Fig. 7
Normalized maximum deflection of the deflected microbeam with half-sine shock with T=1 ms and 1000g shock amplitude actuation in $\zeta = 0$; (a): V_{dc}=2.05 V; (b): V_{dc}=2.10 V.

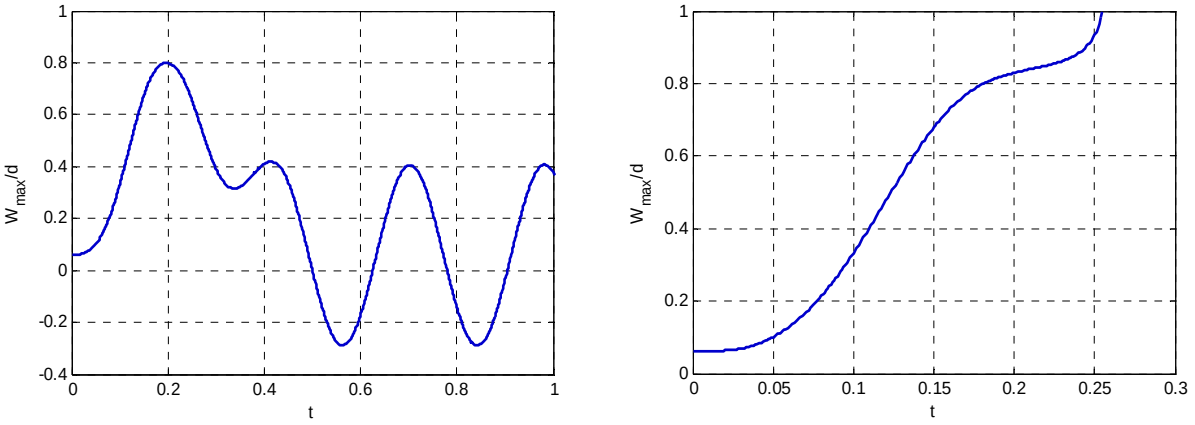

Fig. 8
Normalized maximum deflection of the microbeam under DC and half-sine shock with T=0.1 ms and 1000g shock amplitude actuation in undamped condition; (a): V_{dc}=2.05 V; (b): V_{dc}=2.10 V.

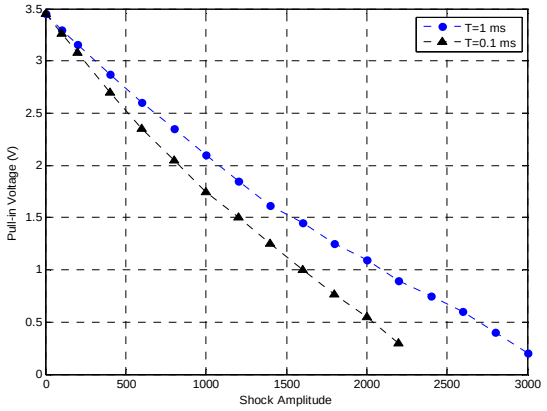

Fig. 9
Pull-in voltage versus half-sine shock amplitude.

So it can be concluded that by decreasing the shock duration, the pull-in voltage decreases. Fig. 9 shows that by increasing the shock amplitude, the pull-in voltage decreases, so that it can be divided in two stable and unstable regions. If the actuation point be placed on the right hand, the system is unstable and if be placed in left hand, the system is stable.

5 CONCLUSION

In the presented work the mechanical behavior of a fixed-fixed microbeam under electrostatic actuation and mechanical shock was investigated. The governing nonlinear elasto-electrostatic equation of the microbeam was derived considering design parameters such as intrinsic residual stress from fabrication processes and the nonlinear stiffening or stretching stress due to beam deflection. Because of the nonlinearity and complexity of the derived static and dynamic equations, they were solved using step by step linearization method and Galerkin based reduced order model, respectively. Then the pull-in voltage of the structure in the case of static actuating by an applied DC voltage was calculated. The effect of shock forces on the mechanical behavior for undeflected and electrostatically deflected micro beam also was studied and shown that the mechanical shock can lead the structure to an unstable position in a lower applied voltage than the static electrostatic pull-in voltages. Also it was shown that by considering stretching stress effect in the governed equation, the microbeam deflection changes non-linearly with the shock amplitude and without this effect, it changes linearly and in small shock amplitudes, the effect of stretching is negligible but in higher shocks this effect is considerable. Finally, it was concluded that by decreasing the shock duration and increasing the shock amplitude, the pull-in voltage decreases.

REFERENCES

[1] Basso M., Giarre L., Dahleh M., Mezic I., 1998, Numerical analysis of complex dynamics in atomic force microscopes, in: *Proceedings of the IEEE International Conference on Control Applications,* Trieste, Italy, 1-4 September: 1026-1030.

[2] Fritz J., Baller M.K., Lang H.P., Rothuizen H., Vettiger P., Meyer E., Gntherodt H.J., Gerber C., Gimzewski J.K., 2001, Translating bio-molecular recognition into nanomechanics, *Science* **288**: 316-318.

[3] Sidles J.A., 1991, Noninductive detection of single proton-magnetic resonance, *Applied Physics Letters* **58**(24): 2854-2856.

[4] Nabian A., Rezazadeh Gh., Haddad-Derafshi M., Tahmasebi A., 2008, Mechanical behavior of a circular micro plate subjected to uniform hydrostatic and non-uniform electrostatic pressure, *Microsystem Technologies* **14**: 235-240.

[5] Senturia S., 2001, *Microsystem Design*, Kluwer, Norwell, MA, USA.

[6] Rezazadeh Gh., Sadeghian H., Abbaspour E., 2008, A comprehensive model to study nonlinear behaviour of multilayered micro beam switches, *Microsystem Technologies* **14**(1): 143.

[7] Sadeghian H., Rezazadeh Gh., Osterberg P.M., 2007, Application of the generalized differential quadrature method to the study of pull-in phenomena of mems switches, *Journal of Microelectromechanical Systems* **16(**6).

[8] Osterberg P.M., Senturia S.D., 1997, M-Test: a test chip for MEMS material property measurement using electrostatically actuated test structures, *Journal of Microelectromechanical Systems* **6**: 107-118.

[9] Abdel-Rahman E.M., Younis M.I., Nayfeh A.H., 2002, Characterization of the mechanical behavior of an electrically actuated microbeam, *Journal of Micromechanical Microengineering* **12**: 759-766.

[10] Younis M.I., Jordy D., Pitarresi J.M., 2007, Computationally efficient approaches to characterize the dynamic response of microstructures under mechanical shock, *Journal of Microelectromechanical Systems* **16**(3).

[11] Tas N., Sonnenberg T., Jansen H., Legtenberg R., Elwenspoek M., 1996, Stiction in surface micromachining, *Journal of Micromechanical Microengineering* **6(**4): 385-397.

[12] Tanner D.M., Walraven J.A., Helgesen K., Irwin L.W., Smith N.F., Masters N., 2000, MEMS reliability in shock environments, in: *Proceedings of the IEEE International Reliability Physics Symposium*, 129-138.

[13] Meirovitch L., 2001, *Fundamentals of Vibrations*, McGraw-Hill, Boston, USA.

[14] Béliveau A., Spencer G.T., Thomas K.A., Roberson S.L., 1999, Evaluation of MEMS capacitive accelerometers, *Design & Test of Computers, IEEE* **16**: 48-56.

[15] Brown T.G., Davis B., Hepner D., Faust J., Myers C., Muller P., Harkins T., Hollis M., Miller C., Placzankis B., 2001, Strapdown microelectromechanical (MEMS) sensors for high-G munition applications, *IEEE Transactions on Magnetics* **37**: 336-342.

[16] Lim B.B., Yang J.P., Chen S.X., Mou J.Q., Lu Y., 2002, Shock analysis of MEMS actuator integrated with HGA for operational and non-operational HDD, In: *Digest of the Asia-Pacific Magnetic Recording Conference*, WE-P-18-01-WE-P-18-02.

[17] Wagner U., Franz J., Schweiker M., Bernhard W., Muller-Fiedler R., Michel B., Paul O., 2001, Mechanical reliability of MEMS-structures under shock load, *Microelectronics Reliability.* **41**: 1657-1662.
[18] Fan M.S., Shaw H.C., Dynamic response assessment for the MEMS accelerometer under severe shock loads, In: *National Aeronautics and Space Administration NASA*, Washington, DC, TP-2001-20997.
[19] Li G.X., Shemansky J.R., 2000, Drop test and analysis on micro-machined structures, *Sensors Actuators A* **85**: 280-286.
[20] Srikar V.T., Senturia S.D., 2002, The reliability of microelectromechanical systems (MEMS) in shock environments, *Journal of Microelectromechanical Systems* **11**: 206-214.
[21] Yee J.K., Yang H.H., Judy J.W., 2003, Shock resistance of ferromagnetic micromechanical magnetometers, *Sensors Actuators A* **103**: 242-252.
[22] Millet O., Collard D., Buchaillot L., 2002, Reliability of packaged MEMS in shock environments: crack and stiction modeling, In: *Design, Test, Integration and Packaging of MEMS/MOEMS*, Cannes, 696-703.
[23] Coster J.D., Tilmans H.C., Van Beek J.T.M., Rijks T.G.S.M., Puers R., 2004, The influence of mechanical shock on the operation of electrostatically driven RF-MEMS switches, *Journal of Micromechanical Microengineering* **14**: 549-554.
[24] Mukherjee T., Fedder G.K., Ramaswamy D., White J., 2000, Emerging simulation approaches for micromachined devices, *IEEE Computer-Aided Design of Integrated Circuits and Systems* **19**: 1572-1589.
[25] Senturia S.D., Aluru N., White J., 1997, Simulating the behavior of MEMS devices, *IEEE Computational Science & Engineering* **4**(1): 30-43.
[26] Gupta R.K., 1997, Electrostatic pull-in test structure design for in-situ mechanical property measurement of microelectromechanical systems (MEMS), PhD dissertation, MIT, Cambridge, MA, 10-27.
[27] Rezazadeh Gh., Tahmasebi A., Zubtsov M., 2006, Application of piezoelectric layers in electrostatic mem actuators: Controlling of pull-in voltage, *Microsystem Technologies* **12**(12): 1163-1170.
[28] Nayfeh A.H., Mook D.T., 1979, *Nonlinear Oscillations*, Wiley, New York.
[29] de Silva Clarence W., 2005, *Vibration and Shock Handbook*, CRC Press, Taylor & Francis Group.